Available online at www.sciencedirect.com

SciVerse ScienceDirect

Ceramics International 38 (2012) 4181–4187

CERAMICS INTERNATIONAL

www.elsevier.com/locate/ceramint

Synthesis and characterization of $Bi_{1.5}Zn_{0.92}Nb_{1.5-x}Sn_xO_{6.92-x/2}$ pyrochlore ceramics

A.F. Qasrawi [a,b,*], Bayan H. Kmail [b], A. Mergen [c]

[a] Group of Physics, Faculty of Engineering, Atilim University, 06836 Ankara, Turkey
[b] Department of Physics, Arab-American University, Jenin, West Bank, Palestine
[c] Metallurgical and Materials Engineering Department, Marmara University, 34722 Istanbul, Turkey

Received 4 August 2011; received in revised form 7 January 2012; accepted 28 January 2012
Available online 4 February 2012

Abstract

The morphological, compositional, structural, dielectric and electrical properties of $Bi_{1.5}Zn_{0.92}Nb_{1.5-x}Sn_xO_{6.92-x/2}$ ceramics have been investigated by means of scanning electron microscopy (SEM), X-ray energy dispersion spectroscopy (EDS), X-ray diffraction (XRD), temperature and frequency dependent dielectric constant and temperature dependent conductivity measurements for Sn-contents in the range of $0.00 \leq x \leq 0.60$. It was shown that single phase of the pyrochlore ceramics can only be obtained for $x \leq 0.25$. Above this value a ZnO phase appeared in the XRD patterns and SEM micrographs as well. An increase in the lattice constant and in the temperature coefficient of dielectric constant and a decrease in the dielectric constant values with increasing Sn content was observed for the ceramics which exhibited a single phase formation. A temperature dependent but frequency invariant dielectric constant was observed for this type of ceramics. The lowest electrical conductivity and highest dielectric constant was observed for the sample which contains 0.06 Sn. The $Bi_{1.5}Zn_{0.92}Nb_{1.5-x}Sn_xO_{6.92-x/2}$ pyrochlore ceramic conductivities are thermally active above 395 K. For temperatures greater than 395 K, the conductivity activation energy which was found to be 0.415 eV for the pure sample increased to 1.371 eV when sample was doped with 0.06 Sn.

PACS : 72.80.Tm; 77.22.Gm; 78.20.Bh

Keywords: B. Structure and microstructure; C. Electrical properties; C. Dielectric properties

1. Introduction

Due to the rapid growth of the wireless communication systems and microwave products in the consumer electronic market, small, light weight and multifunctional electronic components are nowadays attracting much attention. The component manufacturers always look for new advanced integrated and interconnected technologies. One of the suggested solutions is the low temperature cofired ceramic technology which enables design of three-dimensional ceramic modules with low dielectric loss and embedded metal electrodes [1].

Bismuth, zinc and niobium (BZN) based ceramics which exhibits high dielectric constant and low sintering temperatures, belongs to the Class-I dielectric group. The most important compound form in the BZN system is the $Bi_{1.5}Zn_{0.92}Nb_{1.5}O_{6.92}$ (BZN) cubic pyrochlore. BZN pyrochlore has a low sintering temperature below 1000 °C, high relative dielectric permittivity, low dielectric loss and temperature stability [2,3]. Due to its remarkable properties, BZN pyrochlore is a promising material for microelectronic industry as multilayer capacitor and low temperature co-fired ceramics and also for microwave communications as resonator.

Various ions were doped into the BZN to impart different properties to the BZN. For example, Huiling and Xi [4] studied the dielectric relaxation in Ti doped $Bi_{1.5}Zn_{1.0}Nb_{1.5}O_7$ pyrochlore ceramic. Ti incorporation decreased the dielectric relaxation temperature and increased the permittivity of the ceramics. In addition, vanadium metal which was doped into the $Bi_{1.5}Zn_{1.0}Nb_{1.5}O_7$ pyrochlore as sintering aid decreased the sintering temperature to 850 °C [5]. Moreover, Gd incorporation into the A-site of $Bi_{1.5}Zn_{1.0}Nb_{1.5}O_7$ pyrochlore instead of Bi significantly affected the dielectric properties [6].

* Corresponding author. Fax: +90 312 5868091; mobile: +90 972599379412.
E-mail addresses: atef_qasrawi@atilim.edu.tr, aqasrawi@aauj.edu (A.F. Qasrawi).

0272-8842/$36.00
doi:10.1016/j.ceramint.2012.01.079

In our previous works, we have studied the structural, optical [7] and dielectric [8] properties of the pure $Bi_{1.5}Zn_{0.92}Nb_{1.5}O_{6.92}$ ceramics. We have found that the $Bi_{1.5}Zn_{0.92}Nb_{1.5}O_{6.92}$ pyrochlore exhibits an indirect transitions band gap of 3.30 eV [7]. The room temperature refractive index was also determined and analyzed to determine the dispersion and oscillator energies, static and lattice dielectric constants and static refractive index of the pure BZN pyrochlore. In the other work [8], $Bi_{1.5}Zn_{1.0}Nb_{1.5}O_7$ and $Bi_{1.5}Zn_{0.92}Nb_{1.5}O_{6.92}$ pyrochlore compositions were prepared and investigated by X-ray diffraction and scanning electron microscopy and their dielectric properties were measured. XRD of $Bi_{1.5}Zn_{0.92}Nb_{1.5}O_{6.92}$ gave only single phase pyrochlore but second phases were observed in the XRD of $Bi_{1.5}Zn_{1.0}Nb_{1.5}O_7$. The scanning electron microscopy supported X-ray results but in the microstructure of $Bi_{1.5}Zn_{1.0}Nb_{1.5}O_7$ composition a Zn-rich phase was also observed in addition to pyrochlore and ZnO. $Bi_{1.5}Zn_{0.92}Nb_{1.5}O_{6.92}$ pyrochlore had higher dielectric constant and lower loss values than $Bi_{1.5}ZnNb_{1.5}O_7$ composition between 25 °C and 200 °C in the frequency range of 10 kHz to 2 MHz.

For the purpose of improving the electronic performance of the BZN pyrochlore ceramics as promising candidates to be used as microwave multilayer ceramic capacitor which is able to store very high amount of energy in very small size, here in this article, we will discuss the Sn doping effects on this material. Particularly, the Sn incorporation effects on the compositional, structural, dielectric and electrical properties of the $Bi_{1.5}Zn_{0.92}Nb_{1.5}O_{6.92}$ (BZN) pyrochlore. In addition, the effect of the applied ac signal frequency and temperature on the dielectric constant and on the dielectric loss will be examined. Furthermore, the transport properties of the Sn doped microwave ceramics will be investigated by means of electrical conductivity measurements.

2. Experimental details

Sn doped BZN ceramic powders having the composition $Bi_{1.5}Zn_{0.92}Nb_{1.5-x}Sn_xO_{6.92-x/2}$ where $x = 0.0$–0.6 were prepared by the conventional high temperature solid state reaction technique. Starting materials of Bi_2O_3 (99.99%, Aldrich), Nb_2O_5 (99.5%, Merck), ZnO (99.5%, Aldrich) and SnO_2 (99%, Alfa Aesar) were mixed by ball milling for 15 h in ethanol using zirconia balls. After drying, the powders were calcined at 800 °C for 4 h and they were milled in an agate mortar. The powders were pressed into a 10 mm diameter and 1–2 mm thickness disks. They were, then, sintered between 1000 and 1025 °C for 4 h in air in a tightly closed alumina crucible to prevent evaporation losses. X-ray diffraction analysis was performed using an X-ray diffractometer (Rigaku, Cu Kα radiation, 1°/min) using powdered samples and the unit cell parameters were computed by the least square method. The densities of the samples were measured by Archimedes method. SEM (JEOL 5910LV) was used to examine the morphology of the sintered ceramics on fracture surfaces and surface. The dielectric measurements of Sn doped BZN ceramics were performed at frequencies from 1 kHz to 2 MHz on silver-plated discs using a high precision LCR meter (HP 4284A). The temperature dependence of the dielectric properties was measured using an automated system consisting of a PC, a HP 4284 LCR meter and a temperature chamber. The electrical resistivity was measured by a high temperature home made cryostat connected to A Keithely 485 Pico-ammeter and Phywe high voltage source.

The probability of Ag diffusion into the pyrochlore was tested by the current–voltage and capacitance–frequency curves after each heating cycle and at different distant times. No changes in the dielectric and in the resistivity values were observed.

3. Results and discussion

3.1. Structural and compositional analysis

Because the ionic radius of Sn (6 coordination number) element is the same as the radius of Nb ion (0.69 Å), Sn was doped into the B-site of BZN pyrochlore in place of Nb. Sn content at all ratios between $x = 0.0$–0.6 using the formula of $Bi_{1.5}Zn_{0.92}Nb_{1.5-x}Sn_xO_{6.92-x/2}$ resulted in single and multi-phase formation. For x values less than 0.25, the reflected X-ray patterns, presented in Fig. 1, did not show any secondary phase in the structure of the BZN, indicating that replacement of Nb by Sn forms a complete substitutional solid solution. When x is greater than 0.25, the ZnO (second) phase (card number: JCPDS Kart No.: 36-1451) started to form (Fig. 1).

The lattice parameters of the Sn doped BZN pyrochlore ceramics are determined by the least square method and found to be 10.5616, 10.5554, 10.5560 and 10.5598 Å, for x values of 0.00, 0.06, 0.10 and 0.20, respectively. These numerical values suggest an increase in the lattice constant with increasing Sn content. The attenuation of the lattice parameters with Sn content may be attributed to the recrystallization process. However, it should always be noticed that the XRD determines only the average periodic structure and does not offer insights to any local structural distortion.

The inset of Fig. 2 represents the scanning electron microscopy (SEM) image for the BZN sample which contains 0.25 Sn. For point 1 which is shown in that image, the energy

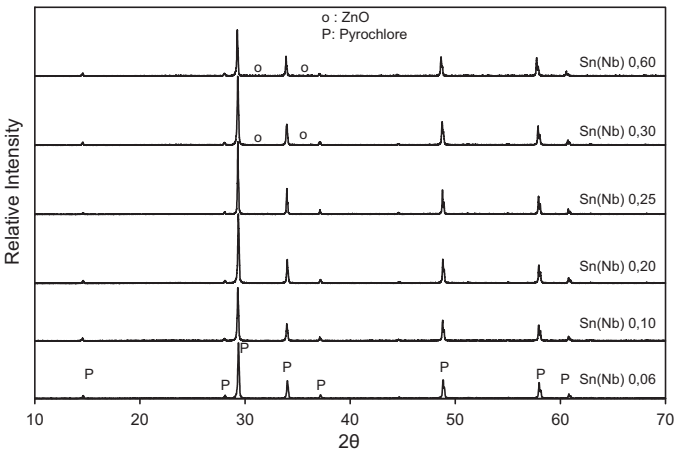

Fig. 1. The X-ray diffraction patterns of the $Bi_{1.5}Zn_{0.92}Nb_{1.5-x}Sn_xO_{6.92-x/2}$ solid solution for $x = 0.06$–0.60.

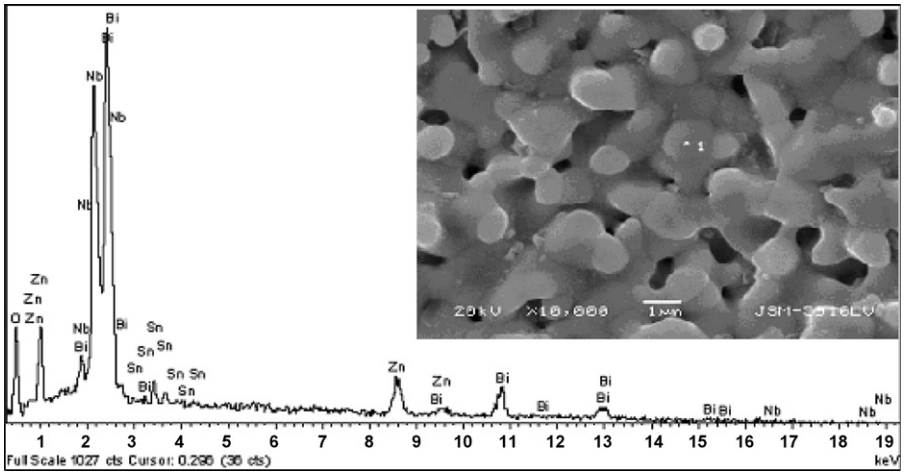

Fig. 2. EDS spectra for of $Bi_{1.5}Zn_{0.92}Nb_{1.25}Sn_{0.25}O_{6.795}$ pyrochlore ceramics. The inset illustrates the backscattered electron image.

dispersive spectroscopy (EDS) analysis illustrated in Fig. 2 shows that the sample contains Bi, Zn, Nb, Sn and O only. The EDS analysis reflected composition ratios of 17.92%, 8.47%, 23.12% 4.57% and 45.92% for O, Zn, Nb, Sn and Bi, respectively. The measured value of Sn content in the sample (4.57%) is close to the theoretically calculated on as (3.96%).

The inset of Fig. 3(a) displays the SEM image for the $Bi_{1.5}Zn_{0.92}Nb_{1.2}Sn_{0.3}O_{6.77}$ samples which contains 0.3 of Sn.

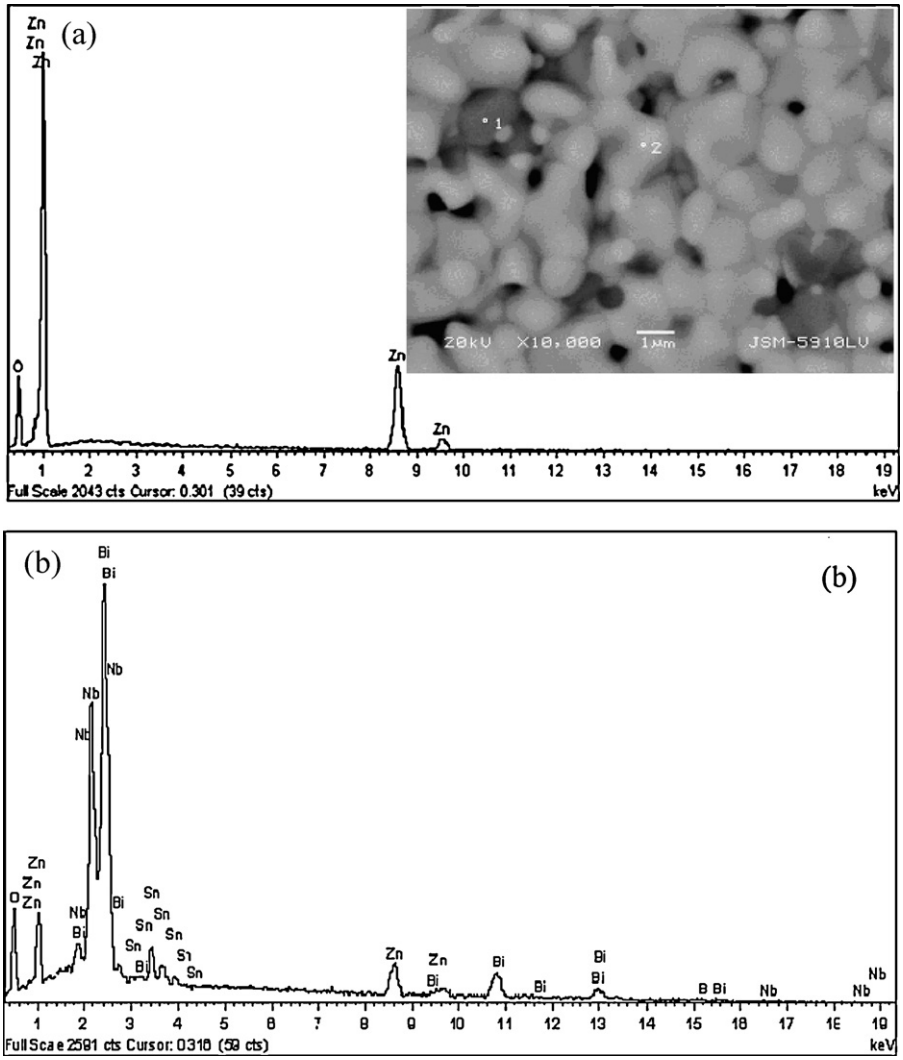

Fig. 3. EDS spectra (a) for ZnO and (b) for $Bi_{1.5}Zn_{0.92}Nb_{1.2}Sn_{0.3}O_{6.77}$ pyrochlore ceramics. The inset of (a) illustrates the backscattered electron image.

Table 1
Structural, dielectric and electrical parameters of Sn doped $Bi_{1.5}Zn_{0.92}Nb_{1.5}O_{6.92}$ ceramics.

x	a^0 (A)	ρ_{th} (g/cm^3)	ρ_B (g/cm^3)	ρ_r (%)	T_s (°C)	ε (0.1 MHz)	tan(δ) ($\times10^{-4}$)	TC (ppm/°C)	σ ($\times10^{-10}(\Omega$ cm)$^{-1}$)
0.00	10.5616	7.11	6.67	93.81	1000	178	8.0	−647	5.08
0.06	10.5554	7.06	6.95	98.5	1025	266	12.5	−493	0.83
0.10	10.5556	7.06	7.05	99.90	1025	207	3.15	−432	0.10
0.20	10.5598	7.08	6.96	98.24	1025	182	7.70	−378	5.82
0.25	10.5524	7.10	7.03	98.98	1000	102	1.78	−385	6.027

Because, some darken points are observable in the image, two different regions shown as points 1 and 2 were selected. The EDS spectra for these two points are shown in Fig. 3(a) and (b). The first point (shown in the image) was found to be composed of 22.19% oxygen and 77.81% zinc only. The second point is composed of 17.33% O, 8.29% Zn, 20.19%Nb, 5.94% Sn, 48.25% Bi. The data indicates the formation of minor phase of ZnO in the BZN pyrochlore for Sn content of 0.3, consistent with the X-ray diffraction results.

The appearance of multiphase in the BZN pyrochlore ceramics was also reported in literature. It has been reported that the pure $Bi_{1.5}Zn_{0.92}Nb_{1.}O_{6.92}$ is always composed of single phase while $Bi_{1.5}ZnNb_{1.5}O_7$ pyrochlore contains very small amount of ZnO phase [8]. Consistent results were also reported by Levin et al. [9] who has analyzed the structure of $Bi_{1.5}ZnNb_{1.5}O_7$ pyrochlore and found that the cubic pyrochlore includes small amount of ZnO. Wu et al. [3] investigated the microstructures of $Bi_{1.5}ZnNb_{1.5}O_7$ and $Bi_{1.5}Zn_{0.92}Nb_{1.5}O_{6.92}$ pyrochlores and proofed that $Bi_{1.5}ZnNb_{1.5}O_7$ was not composed of a single phase pyrochlore but instead, it consists of unusual structure of $Bi_{1.5}Zn_{0.92}Nb_{1.5}O_{6.92}$ and ZnO which is distributed evenly in the grain and at the boundaries.

It is worth notifying that for the purpose of electrical and dielectric measurements Sn doped BZN ceramics were sintered to obtain high density pellets. The sintering temperatures (T_s) and the densities of Sn doped BZN ceramics are given Table 1. The table includes the density measured by Archimedes method (ρ_B) and the theoretical (ρ_{th}) one. The later is calculated from the chemical formula of the composite to obtain the atomic mass and the measured lattice constant from the X-ray diffraction data to obtain the unit cell volume. All the samples were restricted to have relative density (ρ_r) greater than 97%. The samples which exhibited low relative density were improved by raising the sintering temperature.

3.2. Dielectric analysis

The effect of Sn doping on the dielectric constant (ε) is presented in Table 1. As it is readable from the table, the value of the dielectric constant of the pure sample at room temperature is 178. It increases to 266 when Nb is replaced by 0.06 Sn, where it then decreases with increasing Sn content reaching a value of 102 at $x = 0.25$. Fig. 4(a) and (b), reflects the frequency (f) dependence of dielectric constant for the $Bi_{1.5}Zn_{0.92}Nb_{1.5-x}Sn_xO_{6.92-x/2}$ samples doped with 0.06 and 0.25 (the lowest and highest doping ratios of the single phase pyrochlore), respectively, being recorded at different temperatures in the temperature range of 25–200 °C. At all temperatures for the sample which contain 0.06 Sn, the dielectric constant values are observed to be frequency independent. At any

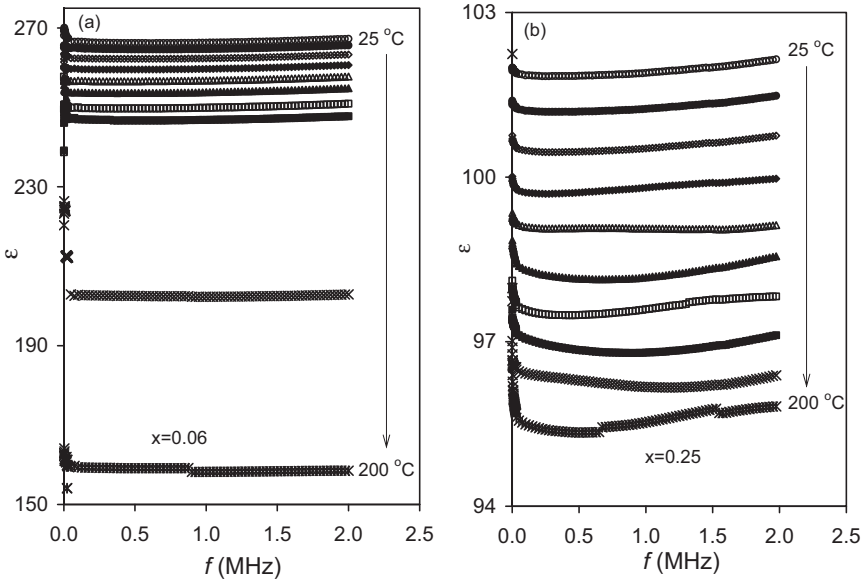

Fig. 4. The frequency dependence of dielectric constant recorded at various temperatures for (a) $Bi_{1.5}Zn_{0.92}Nb_{1.44}Sn_{0.06}O_{6.89}$ and (b) $Bi_{1.5}Zn_{0.92}Nb_{1.25}Sn_{0.25}O_{6.795}$ pyrochlore ceramics.

particular temperature, the dielectric constant value is the same regardless of the applied frequency. The sample which is doped with 0.25 Sn (Fig. 4(b)), reflected a very weak frequency dependence of dielectric constant at temperatures greater than 120 °C. In general, increasing the temperature decreases the value of the dielectric constant. As for example, for one of the presented samples ($x = 0.25$), at 0.1 MHz, the dielectric constant decreases from 102 to ∼96 as temperature is raised from 25 to 200 °C, respectively. Fig. 5(a), represents the temperature variation of dielectric constant being recorded at frequencies of 0.1 MHz for the samples doped with 0.06 and 0.25 Sn. For both samples, the variation of $\varepsilon - T$ is linear and can be presented by the relation $\varepsilon = -0.144T + 270.58$ and $\varepsilon = -0.035T + 102.64$, respectively. The temperature coefficient of dielectric constant, α_ε, which was calculated from the relation $\alpha_\varepsilon = (\varepsilon_{T_2} - \varepsilon_{T_1})/(\varepsilon_{T_1}(T_2 - T_1))$ with T_1 and T_2 being 298 and 393 K, respectively, and displayed in Table 1, was found to increase from −760 in pure BZN to −493 for $x = 0.06$ and reaches −385 ppm/°C at $x = 0.25$.

The decrease in the value of the dielectric constant with temperature may be attributed to the contribution of more than one type of polarization, electronic, ionic, dipolar and space charge polarization. The nature of the variation of the dielectric constant as function of temperature and frequency determines which type of contribution is dominant [10]. Since the dielectric constant is frequency independent as shown in Fig. 4, it indicates no role of applied electric field on the electronic polarization processes. In this region the decrease of dielectric constant with temperature may be mainly due to the contribution of the same type of polarization.

Table 1 displays the Sn content effect on the room temperature dielectric loss (tan(δ)) being recorded at frequency (f) of 0.1 MHz for BZN pyrochlore ceramics. Although the behavior of the dielectric loss with Sn ratio is not systematic, it exhibits an order of magnitude of 10^{-4}–10^{-3} which are relatively low for all the samples under investigation. This property makes the Sn doped ceramics attractive for application in telecommunication electronics. Fig. 5(b) reflects the temperature effect on the dielectric loss being recorded at frequencies of 0.1 MHz for both presented samples. As may be read from this figure, the higher the temperature the greater the dielectric loss value. The increase in the dielectric loss with increasing temperature was also observed for $SrBi_2V_xNb_{2-x}O_9$ ferroelectric ceramics [11]. The behavior of loss values was attributed to the intrinsic defect formation at higher temperatures. The formation of defects in the ceramics structure was assigned to expected bismuth and/or $[Bi_2O_2]^{2-}$ evaporation at high temperatures. For this reason, the samples may have possessed vacancies generating charge carriers [12]. The introduction of V in place of niobium is suggested to ease the release of the charge carriers and therefore the doped samples would show higher loss at higher temperatures.

The values of the dielectric constant determined here lies in the preferable range for radiowave and microwave detection [3,13,14]. The variation of the dielectric constant of $Bi_{1.5}Zn_{0.92}Nb_{1.5-x}Sn_xO_{6.92-x/2}$ pyrochlore ceramics with Sn content, the low dielectric loss of the dielectric constant, the relatively low sintering temperature, the dielectric constant-frequency stability, the linear variation of dielectric constant with temperature, and small light weight of the $Bi_{1.5}Zn_{0.92}Nb_{1.5-x}Sn_xO_{6.92-x/2}$ ceramics make them suitable and attractive multifunctional electronic components that can be implanted in wireless communication technology.

3.3. Electrical conductivity analysis

The Ohmic nature of the electrical contacts was tested in the applied voltage range of 10–300 V. The data of the forward and reverse bias I–V characteristics are shown in the inset of Fig. 6. The inset displays the linear dependence of the voltage on the current for the sample doped with 0.25 Sn. It also reflects the independency of the I–V on biasing direction. All the other studied samples are also observed to be of Ohmic nature for this range of applied voltage.

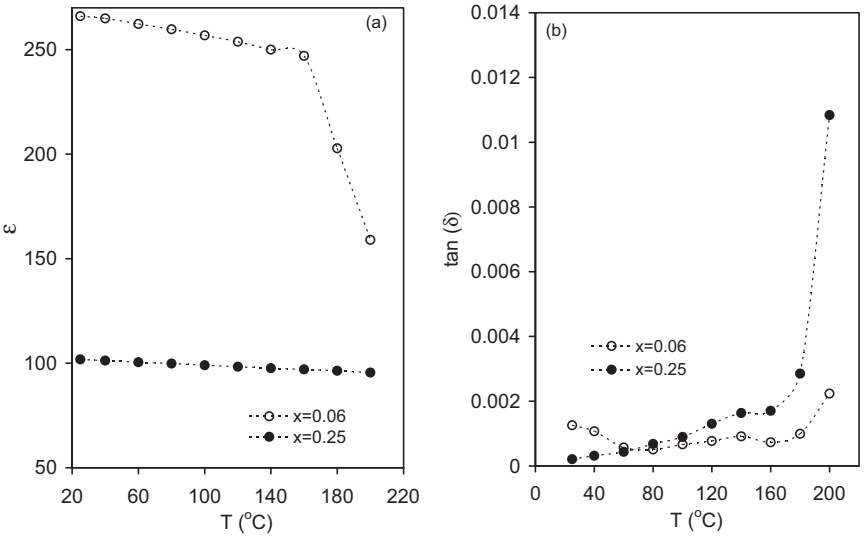

Fig. 5. (a) The ε–T variation of BZN doped with 0.06 and 0.25 Sn. (b) The temperature dependence of the dielectric loss for BZN pyrochlore ceramics.

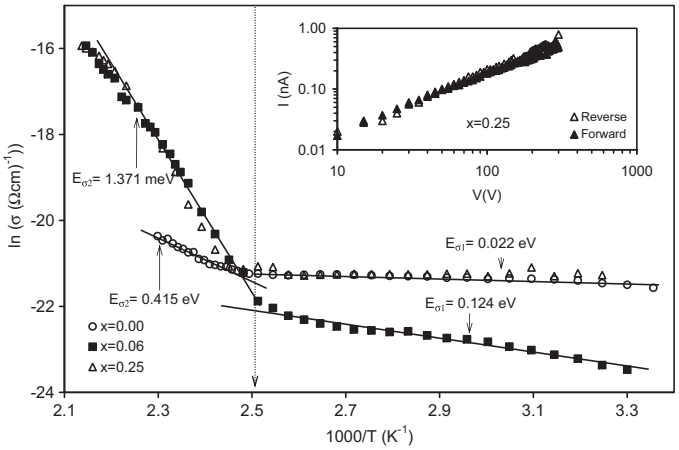

Fig. 6. The $\ln(\sigma) - T^{-1}$ variations for $Bi_{1.5}Zn_{0.92}Nb_{1.5-x}Sn_xO_{6.92-x/2}$ ceramics. The inset illustrates the *I–V* characteristics.

The electrical conductivity was measured by the Hall bar technique. The values of the electrical conductivities (σ) recorded around room temperature are displayed in Table 1. Generally, the electrical conductivities of the samples are very low. While the pure sample exhibits conductivity value of the order of $10^{-10}\ \Omega\ cm^{-1}$, the 0.06 and 0.10 Sn doped samples exhibited lower conductivity values. The difference between these doped and pure samples is approximately in one order of magnitude indicating that although both Sn and Nb have the same ionic radius, they may exhibit different electrical conduction. As may also be seen from Table 1, further increase in Sn-content increased the electrical conductivity and decreased the dielectric constant.

Fig. 6 illustrates the variation of dc electrical conductivity with reciprocal temperature. As seen from the figure, for the samples under investigation, the conductivity increases with increasing temperature. The variation of electrical conductivity with temperature follows different rates in different temperature regions. For both pure and doped samples in the temperature region of 300–395 K, the $\sigma - T^{-1}$ variation is week. In this range of temperature, the values of the electrical conductivity for sample which contains 0.06 Sn is less than that of the pure and it is also less than that which contains 0.25 Sn. In the temperature region of 400–470 K, the dependence of conductivity on temperature is very high for both pure and doped samples. The thermally activated electrical conductivity of the pure and doped samples follows the relation, $\sigma\alpha\ \exp(-E_\sigma/kT)$ where E_σ is the conductivity activation energy. The linear slopes – shown by solid lines in Fig. 6 of the plots of the $\ln(\sigma) - T^{-1}$ allowed the determination of the conductivity activation energies as 0.022 and 0.124 eV below 400 K for the pure and 0.06 Sn doped samples and 0.415 and 1.371 eV above 400 K, for the pure and 0.06 and 0.25 Sn-doped samples, respectively. The values of the conductivity activation energies are less than half of the energy gap [7] indicating the extrinsic nature of conduction. The existence of the 0.022 and 0.415 eV energy levels in the pure samples may be attributed to the intrinsic defects formation. On the other hand, the values of the conductivity activation energies being 0.124 and 1.371 eV are mainly due to the Sn-substitution in the pure samples. The constant electrical conductivity with increasing temperature which was observed for the sample which contains 0.25 Sn in the temperature region of 300–395 K, may indicate that the electrical conductivity is not dominated by the bulk ceramic material but by the resistance of the ceramic-surface contacts in the material. This behavior could have happed due to the increased lattice imperfections associated with the growth of the ZnO phase which become pronounced for x values of 0.30.

The abrupt increase in the values of the conductivity activation energy via Sn doping could possibly be attributed to the shrinkage in the energy gap of the BZN pyrochlore with doping. In a previous work [15] we have discussed the effect of nickel doping on the optical and electrical properties of $Bi_{1.5}Zn_{0.92}Nb_{1.5}O_{6.92}$ ceramics. In that study we have shown that the energy band gap increased from 3.30 to 3.35 and 3.52 eV as the Ni content increases from 0.00 to 0.07 and reaches 0.10, respectively. The widening of the energy gap caused a sharp decrease in the conductivity and changes the type of thermal activation. An increase in conductivity activation energy with increasing Zr content was also observed for $Gd_2Ti_{2-y}Zr_yO_7$. It was attributed to the increase in the degree of correlations among mobile oxygen ions in the oxygen ion diffusion process as the structure become more disordered [16]. Consistently an increase in the conductivity activation energy with increasing aluminum content was also observed for $Al_xGa_{1-x}N$ epilayers. The deepening of the activation energy with increasing Al content was assigned to the band gap and electron effective mass increase [17]. However, in another study, we have found that the Ta doping decreased the activation energy from 1.22 to 0.68 eV as Ta content increased from 0.2 to 0.6 [18]. Such behavior reflected an increase in the carrier density with increasing Ta content that in turn lead to shallower activation energy levels. Thus, doping does not necessarily shrinkage the energy gap and even if it does one may also assign the increase in the activation energy with doping to other reasons like the existence of more than one carrier type in the material.

4. Conclusions

The Sn doping effect on the compositional, structural, dielectric and electrical properties of the $Bi_{1.5}Zn_{0.92}Nb_{1.5}O_{6.92}$

pyrochlore ceramics has been studied. The high Sn content is observed to have pronounced effect on the micro-structural, dielectric and electrical properties of the pyrochlore. A sensitivity of dielectric constant to the Sn-content accompanied with low dielectric loss value is observed. This behavior indicates the tunability of the dielectric constant via Sn doping ratio. At particular Sn content, and specific ac signal, the dielectric constant decreased with increasing temperature. This temperature dependent decrement is also associated with increasing electrical conductivity. The variation of the dielectric constant of $Bi_{1.5}Zn_{0.92}Nb_{1.5-x}Sn_xO_{6.92-x/2}$ pyrochlore ceramics with Sn content, the low dielectric loss of the dielectric constant, the relatively low sintering temperature, the dielectric constant-frequency stability, the linear variation of dielectric constant with temperature, and small light weight of the $Bi_{1.5}Zn_{0.92}Nb_{1.5-x}Sn_xO_{6.92-x/2}$ ceramics make them suitable and attractive multifunctional electronic components that can be implanted in wireless communication technology.

Acknowledgements

This work was supported by The Scientific and Technological Research Council of Turkey (TÜBİTAK) under grant 107M083. The authors would also like to thank the B.Sc. student Ms. Eman M. Nazzal and Hussein A. Abu Je'ib from the Department of Physics at the Arab-American University (Palestine) for their help in the electrical data collection and analysis throughout their graduation project.

References

[1] M.T. Sebastian, H. Jantunen, Low loss dielectric materials for LTCC applications: a review, Int. Mater. Rev. 53 (2008) 57–90.

[2] D.P. Cann, C.A. Randall, T.R. Shrout, Investigation of the dielectric properties of bismuth pyrochlores, Solid State Commun. 100 (1996) 529–534.

[3] M.C. Wu, S. Kamba, V. Bovtun, W.F. Su, Comparison of microwave dielectric behaviour between $Bi_{1.5}Zn_{0.92}Nb_{1.5}O_{6.92}$ and $Bi_{1.5}ZnNb_{1.5}O_7$, J. Eur. Ceram. Soc. 26 (2006) 1889–1893.

[4] D. Huiling, Y. Xi, Dielectric relaxation characteristics of bismuth zinc niobate pyrochlores containing titanium, Physica B 324 (2002) 121–126.

[5] W.F Su, S.C. Lin, Interfacial behaviour between $Bi_{1.5}ZnNb_{1.5}O_7.0.02V_2O_5$ and Ag, J. Eur. Ceram. Soc. 23 (2003) 2593–2596.

[6] M. Valant, P.K. Davies, Crystal chemistry and dielectric properties of chemically substituted $(Bi_{1.5}Zn_{1.0}Nb_{1.5})O_7$ and $Bi_2(Zn_{2/3}Nb_{4/3})O_7$ pyrochlores, J. Am. Ceram. Soc. 83 (2000) 147–153.

[7] A.F. Qasrawi, A. Mergen, Energy band gap and dispersive optical parameters in $Bi_{1.5}Zn_{0.92}Nb_{1.5}O_{6.92}$ pyrochlore ceramics, J. Alloys Compd. 496 (2010) 87–90.

[8] A. Mergen, O. Özyoldas, Preparation and dielectric properties of $Bi_{1.5}Zn_{1.0}Nb_{1.5}O_7$ and $Bi_{1.5}Zn_{0.92}Nb_{1.5}O_{6.92}$ pyrochlore ceramics, Ceram. Silikáty 54 (2010) 31–36.

[9] I. Levin, T.G. Amos, J.C. Nino, T.A. Vanderah, C.A. Randall, M.T. Lanagan, Structural study of an unusual cubic pyrochlore $Bi_{1.5}Zn_{0.92}Nb_{1.5}O_{6.92}$, J. Solid State Chem. 168 (2002) 69–75.

[10] S. Ahmed Farag, I.K. Battisha, M.M. El-Rafaay, Study of dielectric properties of α-alumina doped MnO, CdO, MoO, Ind. J. Pure Appl. Phys. 43 (2005) 446–458.

[11] S. Jain, A.K. Jha, Structural and electrical properties of $SrBi_2V_xNb_{2-x}O_9$ ferroelectric ceramics: effect of temperature and frequency, J. Electroceram. 24 (2010) 58–63.

[12] I. Coondoo, A.K. Jha, S.K. Aggarwal, Enhancement of dielectric characteristics in donor doped Aurivillius $SrBi_2Ta_2O_9$ ferroelectric ceramics, J. Eur. Ceram. Soc. 27 (2007) 253–260.

[13] M.-C. Wu, Y.-C. Huang, W.-F. Su, Silver cofirability differences between $Bi_{1.5}$ $Zn_{0.92}Nb_{1.5}O_{6.92}$ and $Zn_3Nb_2O_8$, J. Eur. Ceram. Soc. 27 (2007) 3017–3021.

[14] M.-C. Wu, Y.-C. Huang, W.-F. Su, Silver cofirable $Bi_{1.5}Zn_{0.92}Nb_{1.5}O_{6.92}$ microwave ceramics containing Cuo-based dopants, Mater. Chem. Phys. 100 (2006) 391–394.

[15] A.F. Qasrawi, E.M. Nazzal, A. Mergen, Structural, optical, electrical and dielectric properties of $Bi_{1.5}Zn_{0.92}Nb_{1.5-x}Ni_xO_{6.92-3x/2}$ solid solution, Adv. Appl. Ceram., in press.

[16] K.L. Ngai, Relaxation and Diffusion in Complex Systems, Springer, New York, 2011, p. 711.

[17] Z.Y. Fan, J.Y. Lin, H.X. Jiang, Recent advances in III-nitride UV materials and devices, Electrochem. Soc. Proc. 2 (2004) 24–33.

[18] A.F. Qasrawi, A. Mergen, Structural electrical and dielectric properties of $Bi_{1.5}Zn_{0.92}Nb_{1.5-x}Ta_xO_{6.92}$ pyrochlore ceramics, Ceram. Int. 38 (2012) 581–587.